

Deep Learning Approaches and Motor Current Signature Analysis in Detection of Broken Rotor Bar Faults

Özgür AYDIN¹ , Erhan AKIN² 

¹ Bingöl University, Informatics Department, Bingöl, Türkiye

² Fırat University, Engineering Faculty, Elazığ, Türkiye

Özgür AYDIN ORCID No: 0000-0001-8130-277X

Erhan AKIN ORCID No: 0000-0001-6476-9255

*Corresponding author: iamozguraydin@gmail.com

(Received: 21.05.2024, Accepted: 23.06.2024, Online Publication: 26.09.2024)

Keywords

Induction Motor,
Fault Diagnosis,
Broken Rotor
Bar,
Vision Transformer
Model,
Image Processing

Abstract: Induction motors are preferred in industrial applications due to their simple and robust structure, cost-effectiveness, self-starting capability, high efficiency, and reliability. However, faults like broken rotor bars occasionally encountered in these motors can lead to reduced performance and increased operating costs. Deep learning models are increasingly being used for the early detection of such faults. These models can recognize complex patterns in motor data to identify potential faults in advance, allowing for timely intervention, extending motor life, and ensuring production continuity. In this study, the diagnosis of broken rotor bars in induction motors was performed using four different deep learning models. Binary classification was conducted based on images obtained from current signals using a pre-existing dataset. The study achieved over 90% accuracy, thereby proving the effectiveness of deep learning models on induction motors.

1

Kırık Rotor Çubuğu Arızalarının Belirlenmesinde Derin Öğrenme Yaklaşımları ve Motor Akım İmza Analizi

Anahtar Kelimeler

Asenkron Motor,
Arıza Teşhisi,
Kırık Rotor
Çubuğu,
Vision Transformer
Model,
Görüntü İşleme

Öz: Asenkron motorlar, endüstriyel uygulamalarda sağladıkları basit ve sağlam yapı, maliyet etkinliği, kendiliğinden başlama kabiliyeti, yüksek verimlilik ve güvenilirlik gibi avantajlarla tercih edilir. Ancak, bu motorlarda zaman zaman karşılaşılan kırık rotor çubuğu gibi arızalar, performans düşüklüğüne ve işletme maliyetlerinin artmasına neden olabilir. Bu tür arızaların erken teşhisi için derin öğrenme modelleri giderek daha fazla kullanılmaktadır. Bu modeller, motor verilerinden karmaşık desenleri tanıyarak potansiyel arızaları önceden belirleyebilir, böylece zamanında müdahale ile motor ömrü uzatılabilir ve üretim sürekliliği sağlanabilir. Bu çalışma dört farklı derin öğrenme modeli kullanılarak asenkron motorlardaki kırık rotor çubuğu teşhisi gerçekleştirilmiştir. Hazır veri seti kullanılan çalışmada akım sinyalleri ile elde edilen görüntüler üzerinden ikili sınıflandırma yapılmıştır. Yapılan çalışma sonucunda %90 üzerinde başarımla sonuçlandırılmıştır. Böylece derin öğrenme modellerinin asenkron motorlar üzerinde etkinliği kanıtlanmıştır.

1. INTRODUCTION

Induction motors are efficient and economical devices that are particularly preferred in industrial applications among electric motors. These motors primarily consist of two main components: the stator and the rotor. The stator, located on the outer part of the motor, comprises windings powered by alternating current (AC). When AC is applied, the stator generates a variable magnetic field. This magnetic field induces electric currents in the

inner component known as the rotor, and these currents produce the torque that causes the rotor to start rotating. However, the rotor cannot fully synchronize with the speed of the stator's magnetic field, a phenomenon known as "slip." This characteristic of the motor gives it the name "asynchronous."

The simple structure, low cost, and minimal maintenance requirements of induction motors make them ideal for a wide range of applications. They are particularly widely

used in equipment such as pumps, fans, air compressors, and conveyor belts, where high reliability and resistance to overload conditions are required. These motors are indispensable elements of industrial automation systems and reduce operational costs by providing energy efficiency [1-4].

Fault types encountered in induction motors generally develop due to mechanical, electrical, or environmental factors. Mechanical issues include bearing damage, shaft bending, and coupling faults; these damages typically result from insufficient lubrication, incorrect installation, or overloading. Electrical faults directly affect the motor's performance due to problems in the electrical supply, such as phase imbalances, voltage drops, and high harmonic content. Moreover, situations like short circuits in the stator windings and overheating caused by environmental factors can also shorten the motor's lifespan and lead to insulation degradation. Broken rotor bars, in particular, are one of the most severe mechanical faults in induction motors. The breaking of rotor bars causes the motor to vibrate abnormally, overheat, and reduce energy efficiency. This type of damage usually results from overloading, material fatigue, or installation errors and can lead to significant performance reductions in the motor. Preventing these issues through regular maintenance and proper usage ensures that the motor operates efficiently and has a long service life [4-6]. To detect and classify the faults described, studies have been conducted using vibration signals [7-20], current signals [21-24], and frequency-based analyses [25].

The early detection of faults in induction motors is vital for improving the motor's reliability and operational efficiency. Various methods used for this purpose help identify any potential issues by monitoring the motor's condition. Vibration analysis reveals mechanical problems by measuring the motor's abnormal vibrations, while the thermography method detects overheating and insulation problems by analyzing the temperature distribution on the motor surface. Ultrasonic inspection identifies cracks or structural degradation inside the motor using ultrasonic waves, and oil analysis shows the motor's internal wear condition by examining the metal particles and chemical components in the motor oil. Motor Current Signature Analysis (MCSA), in particular, stands out in detecting electrical faults. By evaluating abnormalities in the motor current, it identifies critical issues such as stator winding damage and broken rotor bars. The use of MCSA provides a deeper analysis of electrical problems, offering more detailed information compared to other methods and playing a central role in motor maintenance strategies. The effective use of these techniques not only reduces repair and maintenance costs by identifying motor faults at an early stage but also extends the motor's lifespan and improves the overall system performance [26-27].

The use of MCSA method for fault diagnosis in induction motors is quite common. For instance, Akkurt and Arabacı (2019) utilized current signal analysis and artificial neural networks to detect bearing faults in induction motors. In their experiments, current signals

obtained from artificially damaged bearings were examined and compared with signals from healthy bearings. Statistical and spectral features were determined, and the artificial neural network was trained, enabling the classification of bearing faults with an accuracy of 95.3% [28]. In their study, Kaya and Ünsal (2022) used artificial neural network models to detect and classify various faults in a 3 kW wound-rotor induction motor. The motor was tested with different fault combinations and operated under full load. As a result of the tests, the detection and classification of multiple faults were achieved with an 87% success rate. These results demonstrate that the proposed method can be applied effectively [29]. These studies have shown that MCSA is an effective tool for fault detection in induction motors. Additionally, by combining it with advanced techniques such as machine and deep learning, the efficiency of this method can be further enhanced.

In this study, it has been shown that different deep learning methods (Vision Transformer, gMLP, MLP Mixer, FNet) can be successfully applied to current signals for fault diagnosis in induction motors. Among the methods used, the highest accuracy rate achieved was between 100%.

2. METHODOLOGY

2.1. Data Collection

Our study was conducted using the publicly available broken rotor bar dataset. This dataset contains electrical and mechanical signals collected from three-phase induction motors. The data was obtained through tests conducted with varying degrees of broken bar faults in the motor's rotor under different mechanical loads; the dataset also includes data from a faultless rotor. The induction motor used operates at 3-phase, 1 horsepower (hp), 220/380V voltage, 4 poles, and a nominal speed of 1785 rpm. The experimental dataset contains four different fault classes and one healthy condition class. The data is organized according to load conditions at torque values ranging from 0.5 to 4.0 Nm. A total of ten experiments were conducted to create each data group. In this paper, the phase current signal (I_a) was used for analysis. The sampling frequency of the electrical signals was set at 50 kHz, and that of the mechanical vibration signals at 7600 Hz [30].

2.2. Classification Algorithms (Deep Learning Models)

2.2.1. Vision Transformer

Vision Transformer (ViT) is a deep learning model that effectively works in visual tasks by dividing images into fixed-size patches and processing these patches through the attention mechanism of the Transformer. ViT, an adaptation of the Transformer model originally developed for natural language processing, performs at a level comparable to the best available CNN models, especially when trained on large-scale datasets. The model creates visual representations by considering the

global context, providing comprehensive learning processes [31-32].

2.2.2. gMLP

gMLP (Gated Multi-Layer Perceptron) is an artificial neural network structure developed as an alternative to Transformer models, incorporating gated units and not relying on attention mechanisms. This model aims to effectively capture interactions between data points by adding gates that control information flow between traditional multilayer perceptrons. gMLP is particularly notable because it is more computationally efficient and requires fewer parameters [33-34].

2.2.3. MLP-Mixer

MLP-Mixer is an innovative deep learning architecture introduced by Google Brain that learns visual representations solely using multilayer perceptrons (MLPs) without resorting to attention mechanisms or convolutional layers. The model first divides the image into patches and then processes these patches using two types of MLPs: one designed to capture interactions across patches (along channels) and another within patches (across patches). This approach allows the MLP-Mixer to handle spatial and feature-based information separately, and it can achieve high performance when trained on large datasets [35-37].

2.2.4. F-Net

F-Net is a deep learning model that does not use an attention mechanism but instead relies on Fourier transformations. It replaces the computationally expensive self-attention layers of the original Transformer model with simple Fourier transformation operations, performing frequency analysis on the data. This allows F-Net to offer a more computationally efficient alternative for natural language processing and other sequential modeling tasks. F-Net's performance can approach that of models trained using attention mechanisms in some tasks while operating much faster and using fewer resources. The model's benefit is particularly notable in large datasets and situations requiring the processing of long sequences [38].

2.3. Performance Metrics

Deep learning performance metrics are used to determine how models perform in classification or regression tasks. Among these metrics: Accuracy shows the percentage of correct predictions among all predictions. Precision indicates how much of a predicted class actually belongs to that class. Recall shows the proportion of actual positives that were correctly predicted. F1 Score is calculated as the harmonic mean of precision and recall and represents the balanced performance of the model. ROC Curve and AUC Value evaluate a classifier's performance from a broader perspective. In this study, metrics such as accuracy, precision, recall, F1 score, and ROC AUC value were used to measure the classification capabilities of deep

learning models. These metrics reveal the model's overall accuracy, reliability, and efficiency in detail. Accuracy, precision, recall formulas are given in equations 1-3.

$$Accuracy = \frac{TP + TN}{TP + TN + FP + FN} \quad (1)$$

$$Precision = \frac{TP}{TP + FP} \quad (2)$$

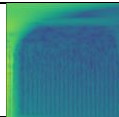
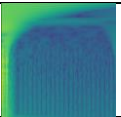
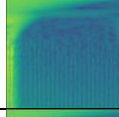
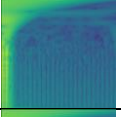
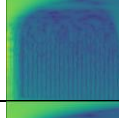
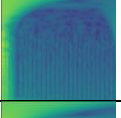
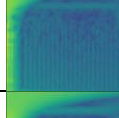
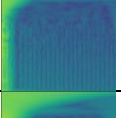
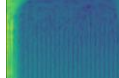

$$Recall = \frac{TP}{TP + FN} \quad (3)$$

3. EXPERIMENTAL STUDIES

During the studies, powerful hardware resources were used for data processing and model training. Specifically, a computer with an Intel Xeon E5-2630 v3 processor and 64 GB RAM was chosen. For running deep learning algorithms, the NVIDIA RTX A5000 GPU with 45 GB RAM was utilized. The stages of reading data from the dataset and processing images were carried out using MATLAB, while the deep learning models were implemented through the Python programming language and its specialized libraries. This hardware and software infrastructure ensured that the study was conducted efficiently and effectively.

In this study, images were generated from the Ia current signals in the dataset. The duration of each signal was set to 18 seconds, and analysis was conducted using non-overlapping windows of 1 second each, between 11 and 15 seconds. With this method, 400 time-frequency representations were obtained for each class of Ia signals under a 0.5 Nm load, resulting in a total of 2000 representations. These representations are presented in Table 1 under five different groups. The image creation process followed the procedural steps taken from the experimental studies conducted by Dişli and colleagues in 2023 [39]. This method provided a detailed framework for signal analysis and interpretation, forming the basis of experimental studies.

Table 1. Time-Frequency Representations Obtained from Ia Data

	400 Sample			
Healthy		...		
Broken Bar 1		...		
Broken Bar 2		...		
Broken Bar 3		...		
Broken Bar 4		...		

In the following sections of our study, we will evaluate the performance of different deep learning models. In this process, binary classification analysis was performed using four different deep learning models. Our dataset consists of images of healthy and unhealthy rotor currents. In total, there are 400 healthy images versus 1600 unhealthy images. This significant imbalance could potentially lead to problems during model training. To address this imbalance, the dataset was restructured. First, 400 images of healthy rotor currents were selected directly. From the unhealthy group, 100 images were randomly selected from each of the four different subgroups, all containing broken rotor bars. With this selection, each unhealthy subgroup was equally represented, resulting in a total of 400 unhealthy images. Consequently, for binary classification analysis, a balanced dataset containing an equal number of images (400 each) from both healthy and unhealthy groups was created. This approach allows the model to generalize training data better and minimize biases that could arise from imbalanced data distribution.

In our study, the deep learning models gMLP, MLP Mixer, and FNet were used alongside ViT. Figure 2 shows the architecture of the ViT deep learning model. In this model, images of 224x224 pixels are divided into patches of 32x32 pixels. Each image contains a total of 49 patches, meaning that patches are repeated seven times along each dimension of the image. Each patch contains a total of 3,072 data points, indicating that each pixel has three color channels, and thus each patch contains $32 \times 32 \times 3 = 3,072$ elements. These structural details provide a fundamental framework for understanding how the model processes images.

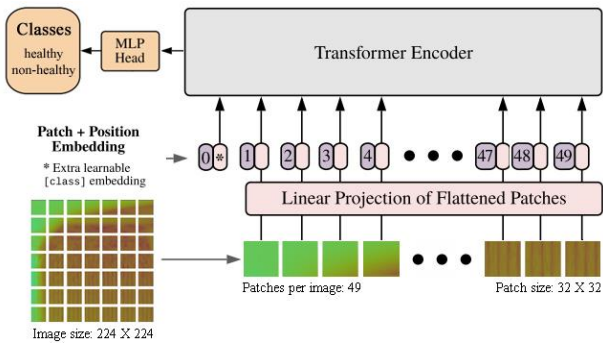


Figure 1. Fault Detection Using the ViT Model

The other deep learning models we used in our study are structurally similar deep learning models. Therefore, the gMLP deep learning model, which achieved the highest performance in our study, is shown in Figure 3. This deep learning model resizes the input images to 512x512 pixels. The model extracts patches from these images with a size of 32x32 pixels and works on each patch. This patch size allows the image to be divided into smaller, manageable parts, enabling the model to learn more detailed and local features on these patches. In total, $(512 / 32)^2$, which is 256 patches are obtained from each image, allowing the model to process a wider image in more detail. Each patch is then transformed into a 256-dimensional embedding vector.

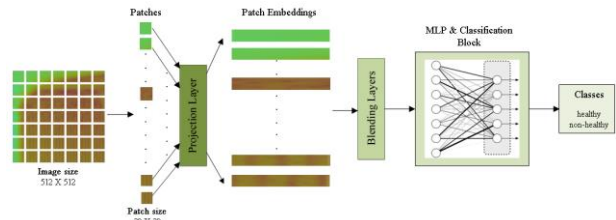
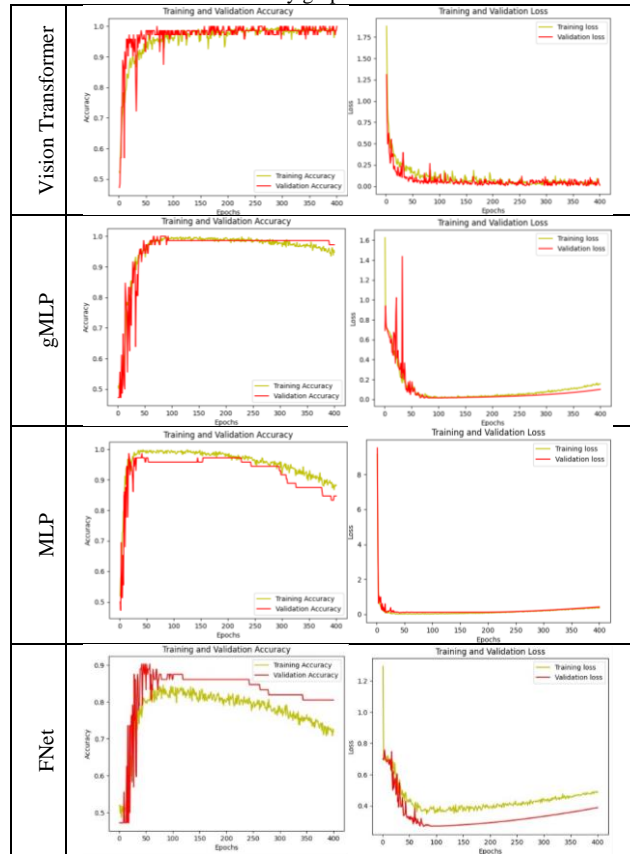


Figure 2. Representation of the gMLP model for fault diagnosis

The training process for all models lasted a total of 400 epochs. Additionally, a dropout rate of 20% was applied to prevent overfitting of the model. These parameters play a significant role in both the configuration and training process of the model.

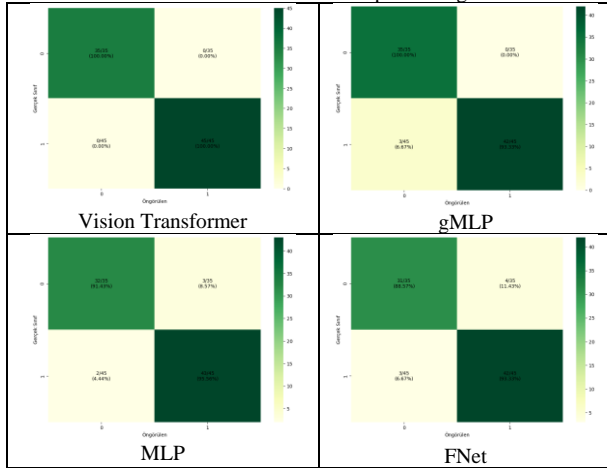
Table 2. The Loss and Accuracy graphs



The Loss and Accuracy graphs of the models examined are presented in Table 2. The Vision Transformer (ViT) model accurately performed all classifications, as documented by the Confusion Matrix. Additionally, this model began to exhibit stable performance after approximately the 100th epoch. When examining the gMLP model, three healthy samples were mistakenly classified as unhealthy. This model began to make stable predictions from the 100th epoch but experienced performance declines after the 250th epoch. The MLP model, on the other hand, generally showed successful performance, making accurate predictions after the 50th epoch, but inconsistencies and performance declines occurred after the 150th epoch. This situation was confirmed by the Confusion Matrix, where four unhealthy samples were classified as healthy, and three healthy samples were classified as unhealthy. The FNet model stands out as the only model that did not show

stable performance throughout the study. Due to the fluctuations in both the accuracy and loss graphs of this model, it was concluded that it did not demonstrate sufficient performance in this study.

Table 3. Confusion Matrix Results of Deep Learning Models



The confusion matrix results of the study are presented in Table 3. In Table 4, the performance metrics for each model have been calculated and interpreted according to the following formulas. **The Vision Transformer** has demonstrated excellent performance with 100% accuracy, precision and recall.

$$\text{Accuracy} : \frac{TP+TN}{TP+TN+FP+FN} = \frac{35+45}{35+45+0+0} = 1.00 \text{ (%100\%)}$$

$$\text{Precision} : \frac{TP}{TP+FP} = \frac{35}{35+0} = 1.00 \text{ (%100\%)}$$

$$\text{Recall} : \frac{TP}{TP+FN} = \frac{35}{35+0} = 1.00 \text{ (%100\%)}$$

gMLP has demonstrated quite good performance with an accuracy rate of 96.25%. The precision value is 92.1% and the recall value is 100%.

$$\text{Accuracy} : \frac{TP+TN}{TP+TN+FP+FN} = \frac{35+42}{35+42+3+0} = \frac{77}{80} = 0.9625$$

$$\text{Precision} : \frac{TP}{TP+FP} = \frac{35}{35+3} = \frac{35}{38} = 0.921$$

$$\text{Recall} : \frac{TP}{TP+FN} = \frac{35}{35+0} = 1.00 \text{ (%100\%)}$$

MLP is performing with an accuracy rate of 93.75%. The precision value is 94.1% and the recall value is 91.4%.

$$\text{Accuracy} : \frac{TP+TN}{TP+TN+FP+FN} = \frac{32+43}{32+43+2+3} = \frac{75}{80} = 0.9375$$

$$\text{Precision} : \frac{TP}{TP+FP} = \frac{32}{32+2} = \frac{32}{34} = 0.941$$

$$\text{Recall} : \frac{TP}{TP+FN} = \frac{32}{32+3} = \frac{32}{35} = 0.914$$

FNet is performing with an accuracy rate of 91.25%. The precision value is 91.2% and the recall value is 88.6%.

$$\text{Accuracy} : \frac{TP+TN}{TP+TN+FP+FN} = \frac{31+42}{31+42+3+4} = \frac{77}{80} = 0.9125$$

$$\text{Precision} : \frac{TP}{TP+FP} = \frac{31}{31+3} = \frac{31}{34} = 0.912$$

$$\text{Recall} : \frac{TP}{TP+FN} = \frac{31}{31+4} = \frac{31}{35} = 0.886$$

Other metrics and all results are provided in Table 4.

Table 4. Performance Metrics of Deep Learning Models

Model	Accuracy	precision	recall	F1 score	Cohens Kappa	ROC AUC
Vision Transformer	%100	1.00	1.00	1.00	1.00	1.00
gMLP	%96,25	0.921	1.00	0.959	0.925	0.967
MLP mixer	%93,75	0.941	0.914	0.927	0.875	0.933
FNet	%91,25	0.912	0.886	0.899	0.825	0.909

In Table 4, the performance metrics of four different deep learning models—Vision Transformer, gMLP, MLP and FNet are examined comparatively. The Vision Transformer model achieved perfect values (1.00) in accuracy, precision, and recall, with an accuracy rate of 100%. This indicates that the model classified all examples in the test set flawlessly. The gMLP model demonstrated very high performance with an accuracy rate of 96.25%, achieving precision and recall values of 0.921 and 1.00, respectively. Additionally, it has a high F1 score of 0.959 and a ROC AUC value of 0.967, indicating the model's balance in classification and overall success as a classifier. The MLP model, with an accuracy of 93.75%, precision of 0.941, and recall of 0.914, showed slightly lower performance compared to the gMLP model. Nevertheless, the F1 score of 0.927 and the ROC AUC value of 0.933 indicate that the model is still a strong classifier. The FNet model, which performed lower than the other three models, has an accuracy rate of 91.25%. However, its precision value of 0.912 shows a high level of correct positive predictions. The recall value of 0.886 indicates a weakness in detecting positive class examples, while the F1 score of 0.899 and the ROC AUC value of 0.909 demonstrate that the model can still deliver acceptable performance under limited conditions.

4. RESULTS

Bu In this study, deep learning models that have recently gained prominence such as ViT, gMLP, MLP Mixer, and FNet were used to perform fault diagnosis on a preprocessed dataset based on current information from electrical motors. These data were analyzed to classify motor conditions as "healthy" and "unhealthy". Experimental results indicated that the Vision Transformer model outperformed the other models; this observation is supported by the stability of the model and its remarkable accuracy rate of 100%. These findings suggest that Vision Transformer is a promising candidate for real-time fault diagnosis applications in electric motors. Particularly, the role this technology could play in the development of real-time fault detection and preventive maintenance strategies could enhance efficiency in industrial processes, thus reducing operational costs. Further studies aim to explore in more detail how effective this model can be under real-world conditions using current and vibration data obtained from asynchronous motors. This could provide valuable insights not only for fault diagnosis but also for process optimization and resource management.

REFERENCES

- [1] Pelly, Brian R. "Thyristor phase-controlled converters and cycloconverters: operation, control, and performance." (No Title) (1971).
- [2] Hughes, Austin, and Bill Drury. *Electric motors and drives: fundamentals, types and applications*. Newnes, 2019.
- [3] Nasar, Syed A., and Ion Boldea. "The induction machine handbook." *Electric Power Engineering Series*, Boca raton, Florida, USA: CRC Press LLC (2002).
- [4] Sen, Paresh Chandra. *Principles of Electric Machines and Power Electronics*, International Adaptation. John Wiley & Sons, 2021.
- [5] Pillay, Pragasen, and Ramu Krishnan. "Modeling, simulation, and analysis of permanent-magnet motor drives. I. The permanent-magnet synchronous motor drive." *IEEE Transactions on industry applications* 25.2 (1989): 265-273.
- [6] Singh, Arvind, et al. "A review of induction motor fault modeling." *Electric Power Systems Research* 133 (2016): 191-197.
- [7] Jing, Luyang, et al. "A convolutional neural network based feature learning and fault diagnosis method for the condition monitoring of gearbox." *Measurement* 111 (2017): 1-10.
- [8] Lou, Xinsheng, and Kenneth A. Loparo. "Bearing fault diagnosis based on wavelet transform and fuzzy inference." *Mechanical systems and signal processing* 18.5 (2004): 1077-1095.
- [9] Zhu, Huibin, et al. "Bearing fault feature extraction and fault diagnosis method based on feature fusion." *Sensors* 21.7 (2021): 2524.
- [10] Banerjee, Tribeni Prasad, and Swagatam Das. "Multi-sensor data fusion using support vector machine for motor fault detection." *Information Sciences* 217 (2012): 96-107.
- [11] Bera, Arka, Arindam Dutta, and Ashis K. Dhara. "Deep learning based fault classification algorithm for roller bearings using time-frequency localized features." *2021 International Conference on Computing, Communication, and Intelligent Systems (ICCCIS)*. IEEE, 2021.
- [12] Lu, Chen, Zhenya Wang, and Bo Zhou. "Intelligent fault diagnosis of rolling bearing using hierarchical convolutional network based health state classification." *Advanced Engineering Informatics* 32 (2017): 139-151.
- [13] Janssens, Olivier, et al. "Convolutional neural network based fault detection for rotating machinery." *Journal of Sound and Vibration* 377 (2016): 331-345.
- [14] Shen, Sheng, et al. "A physics-informed deep learning approach for bearing fault detection." *Engineering Applications of Artificial Intelligence* 103 (2021): 104295.
- [15] Hu, Jie, and Sier Deng. "Rolling bearing fault diagnosis based on wireless sensor network data fusion." *Computer communications* 181 (2022): 404-411.
- [16] Oh, Jin Woo, and Jongpil Jeong. "Data augmentation for bearing fault detection with a light weight CNN." *Procedia Computer Science* 175 (2020): 72-79.
- [17] Chen, ZhiQiang, Chuan Li, and René-Vinicio Sanchez. "Gearbox fault identification and classification with convolutional neural networks." *Shock and Vibration* 2015 (2015).
- [18] Liu, Shuangjie, et al. "Bearing fault diagnosis based on improved convolutional deep belief network." *Applied Sciences* 10.18 (2020): 6359.
- [19] Sun, Wenjun, et al. "A sparse auto-encoder-based deep neural network approach for induction motor faults classification." *Measurement* 89 (2016): 171-178.
- [20] Kumar, Dileep, et al. "Towards soft real-time fault diagnosis for edge devices in industrial IoT using deep domain adaptation training strategy." *Journal of Parallel and Distributed Computing* 160 (2022): 90-99.
- [21] Kao, I-Hsi, et al. "Analysis of permanent magnet synchronous motor fault diagnosis based on learning." *IEEE Transactions on Instrumentation and Measurement* 68.2 (2018): 310-324.
- [22] Hoang, Duy Tang, and Hee Jun Kang. "A motor current signal-based bearing fault diagnosis using deep learning and information fusion." *IEEE Transactions on Instrumentation and Measurement* 69.6 (2019): 3325-3333.
- [23] Aydin, İlhan, Mehmet Karakose, and Erhan Akin. "An approach for automated fault diagnosis based on a fuzzy decision tree and boundary analysis of a reconstructed phase space." *ISA transactions* 53.2 (2014): 220-229.
- [24] Ince, Turker, et al. "Real-time motor fault detection by 1-D convolutional neural networks." *IEEE Transactions on Industrial Electronics* 63.11 (2016): 7067-7075.
- [25] Jia, Feng, et al. "Deep neural networks: A promising tool for fault characteristic mining and intelligent diagnosis of rotating machinery with massive data." *Mechanical systems and signal processing* 72 (2016): 303-315.
- [26] Bonnett, Austin H. "Root cause AC motor failure analysis with a focus on shaft failures." *IEEE transactions on industry applications* 36.5 (2000): 1435-1448.
- [27] Thomson, William T., and Ronald J. Gilmore. "Motor Current Signature Analysis To Detect Faults In Induction Motor Drives-Fundamentals, Data Interpretation, And Industrial Case Histories." *Proceedings of the 32nd turbomachinery Symposium*. Texas A&M University. Turbomachinery Laboratories, 2003.
- [28] Akkurt, İbrahim, and Hayri Arabacı. "Sürücüden Beslenen Asenkron Motorlarda Rulman Arızalarının Stator Akımı Kullanarak Tespiti." *Uluslararası Doğu Anadolu Fen Mühendislik ve Tasarım Dergisi* 1.2 (2019): 122-134.
- [29] Kaya, Kadir, and Abdurrahman Ünsal. "Yapay sinir ağlarıyla asenkron motor çoklu arızalarının tespiti ve sınıflandırılması." *Politeknik Dergisi* 25.4 (2022): 1687-1699.
- [30] Treml, Aline Elly, et al. "Experimental database for detecting and diagnosing rotor broken bar in a

- three-phase induction motor." *IEEE DataPort* (2020).
- [31] Dosovitskiy, Alexey, et al. "An image is worth 16x16 words: Transformers for image recognition at scale." *arXiv preprint arXiv:2010.11929* (2020).
- [32] Khan, Salman, et al. "Transformers in vision: A survey." *ACM computing surveys (CSUR)* 54.10s (2022): 1-41.
- [33] Liu, Hanxiao, et al. "Pay attention to mlps." *Advances in neural information processing systems* 34 (2021): 9204-9215.
- [34] Gorishniy, Yury, et al. "Revisiting deep learning models for tabular data." *Advances in Neural Information Processing Systems* 34 (2021): 18932-18943.
- [35] Tolstikhin, Ilya O., et al. "Mlp-mixer: An all-mlp architecture for vision." *Advances in neural information processing systems* 34 (2021): 24261-24272.
- [36] Melas-Kyriazi, Luke. "Do you even need attention? a stack of feed-forward layers does surprisingly well on imagenet." *arXiv preprint arXiv:2105.02723* (2021).
- [37] Hou, Qibin, et al. "Vision permutator: A permutable mlp-like architecture for visual recognition." *IEEE transactions on pattern analysis and machine intelligence* 45.1 (2022): 1328-1334.
- [38] Lee-Thorp, James, et al. "Fnet: Mixing tokens with fourier transforms." *arXiv preprint arXiv:2105.03824* (2021).
- [39] Dişli, Fırat, Mehmet Gedikpınar, and Abdulkadir Sengur. "Deep transfer learning-based broken rotor fault diagnosis for Induction Motors." *Turkish Journal of Science and Technology* 18.1 (2023): 275-290.